

Changing the Direction of Flagellar Rotation in Bacteria by Modulating the Ratio between the Rotational States of the Switch Protein FliM

Anat Bren and Michael Eisenbach*

Department of Biological
Chemistry, The Weizmann
Institute of Science
76100 Rehovot, Israel

One of the major questions in bacterial chemotaxis is how the switch, which controls the direction of flagellar rotation, functions. It is well established that binding of the signaling molecule CheY to the switch protein FliM shifts the rotation from the default direction, counterclockwise, to clockwise. How this shift is done is still a mystery. Our aim in this study was to determine the correlation between the fraction of FliM molecules in the clockwise state (i.e. occupied by CheY) and the probability of clockwise rotation. For this purpose we gradually expressed, from a plasmid, a clockwise FliM mutant protein in cells that express, from the chromosome, wild-type FliM but no chemotaxis proteins. We verified that plasmid-borne FliM exchanges chromosomal FliM in the switch. Surprisingly, a substantial clockwise probability was not obtained before the large majority of the FliM molecules in the switch were clockwise molecules. Thereafter, the rise in clockwise probability was very steep. These results suggest that an increase in the clockwise probability requires a high level of FliM occupancy by CheY $\sim P$. They further suggest that the steep increase in clockwise rotation upon increasing CheY levels, reported in several studies, is due, at least in part, to cooperativity of post-binding interactions within the switch. We also carried out the inverse experiment, in which wild-type FliM was gradually expressed in a background of a clockwise *fliM* mutant. In this case, the level of the clockwise mutant protein, required for establishing a certain clockwise probability, was lower than in the original experiment. If our system (in which the ratio between the rotational states of FliM in the switch is established by slow exchange) and the native system (in which the ratio is established by fast changes in FliM occupancy) are comparable, the results suggest that hysteresis is involved in the switch function. Such a situation might reflect a damping mechanism, which prevents a situation in which fluctuations in the phosphorylation level of CheY throw the switch from one direction of rotation to the other.

© 2001 Academic Press

*Corresponding author

Keywords: chemotaxis; CheY; flagellar rotation; flagellar switch; FliM

Introduction

Bacteria such as *Escherichia coli* and *Salmonella enterica* serovar Typhimurium swim by rotating their flagella (five to ten flagella per cell). Each flagellum is driven by a motor located at its base and embedded in the cytoplasmic membrane. The direction of flagellar rotation determines the swim-

ming behavior of the cell (see Macnab¹ for a review on bacterial flagella and motility). Thus, the essence of bacterial chemotaxis is modulation of the direction of flagellar rotation.²

A key element in controlling the direction of flagellar rotation is the switch of the flagellar motor (for a review, see Macnab³). This is essentially a "gear box" that receives signals from the chemotaxis receptors and modulates the direction of flagellar rotation accordingly. The switch extends from the base of the flagellar motor (termed basal body) into the cytoplasm. It is composed of three proteins: FliG (~ 35 molecules per switch^{4,5}), FliM

Abbreviations used: CCW, counterclockwise; CW, clockwise.

E-mail address of the corresponding author:
m.eisenbach@weizmann.ac.il

(~ 35 molecules^{4,5}), and FliN (~ 100 molecules⁶). The mechanism underlying the switch function is still a mystery.

The default direction of flagellar rotation is counterclockwise (CCW),^{7,8} resulting in swimming in a rather straight line. The probability of rotation in the other direction, clockwise (CW), increases in response to a negative sensory stimulation (an increased gradient of a repellent or a decreased gradient of an attractant).² This sensory information, sensed by the receptors, is transduced to the switch by the chemotaxis-signaling cascade (see reviews⁹⁻¹²). It involves phosphorylation of the response regulator CheY by its histidine kinase CheA.¹³⁻¹⁵ Phosphorylated CheY (CheY \sim P) binds to the switch protein FliM¹⁶ with a consequent increased probability of CW rotation.¹⁷ This change in the direction of flagellar rotation results in an abrupt turning motion (tumbling) of the cell, after which it swims in a new direction.^{2,18-21}

While the mechanism of signal propagation ending at CheY activation by phosphorylation is relatively well understood, the processes that occur subsequent to CheY \sim P-FliM binding are not known. For example, it is not known how many FliM molecules at the switch should be occupied by CheY \sim P for generating CW rotation. Furthermore, while it is known that CW rotation increases steeply and cooperatively with the intracellular concentration of CheY \sim P,²²⁻²⁵ it is not known whether CheY \sim P binding *per se* or the subsequent switching event is the cooperative step. Our aim in this study was to address these open questions.

Results

Rationale

The main aim of this study, to determine the correlation between the fraction of FliM molecules occupied by CheY \sim P and the probability of clockwise rotation, is very difficult to address directly. We therefore took an indirect approach. It is con-

ceivable that, in the absence of CheY, FliM is in its default CCW state and that, upon CheY \sim P binding, it acquires a CW state. We assumed that we can use molecules of wild-type FliM (FliM_{WT}) in the absence of CheY as representatives of wild-type FliM molecules in their CCW state, and FliM molecules of a CW *fliM* mutant (FliM_{CW}) as representatives of CheY \sim P-occupied, wild-type FliM molecules in their CW state. Our idea was to generate switch complexes with different ratios between FliM_{WT} and FliM_{CW} and to determine the correlation between the ratio of the proteins and the direction of flagellar rotation (Figure 1). We accomplished this by co-expressing the proteins (one from the chromosome and one from a plasmid) in a strain that lacks the response regulator CheY. We wished to assure that the different ratios between FliM_{WT} and FliM_{CW} are mainly established by exchange of FliM molecules within pre-existing switch complexes rather than by synthesis of new flagella. We therefore induced the plasmid-containing cells for not more than three generations (the time required for synthesis of a new flagellum²⁶).

Generation of strains expressing modulatable levels of FliM_{CW} or FliM_{WT}

To obtain different FliM_{WT}/FliM_{CW} ratios, we gradually produced FliM_{CW} from a tightly regulated plasmid in a gutted strain (a strain lacking all the cytoplasmic chemotaxis protein²⁷) expressing endogenous FliM_{WT}. Alternatively, we gradually produced FliM_{WT} in a gutted strain expressing endogenous FliM_{CW}. As a first step in strain construction, we looked for a *fliM* mutant strain, whose flagella rotate predominantly CW in a CheY-independent manner and which would serve as both a source for FliM_{CW} and a host for FliM_{WT} expression. We examined the rotational bias of five *Salmonella* mutant strains, which had been identified as *cheY* suppressors with strong tumbly phe-

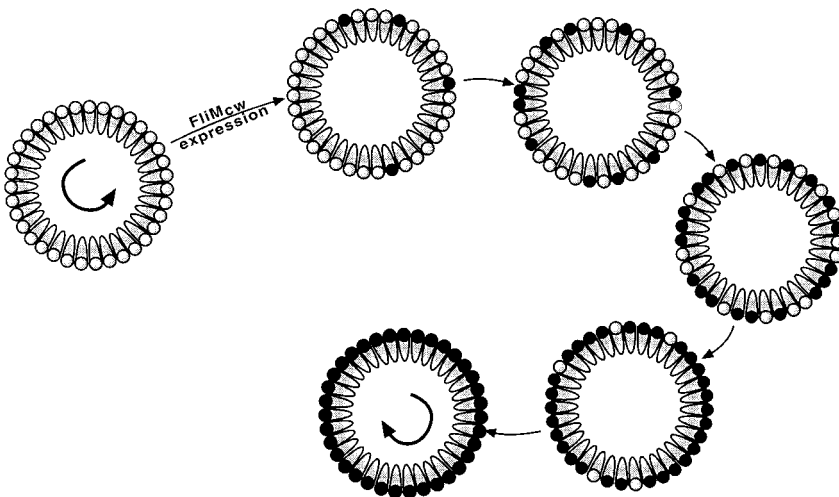


Figure 1. Schematic presentation of a gradual increase in FliM_{CW} level in a flagellar switch of a gutted strain, containing FliM_{WT} molecules. By gradual expression of FliM_{CW} from a tightly regulated plasmid in a gutted strain that expresses endogenous FliM_{WT}, the switch is modulated from a situation, in which all the FliM molecules are in their CCW state, to a situation, in which they are in their CW state. Filled circles, FliM_{CW}; open circles, FliM_{WT}.

notypes and which have normal flagellation and motility: *fliM*(60RC), (70FL), (81VE), (181RH), and (181RP) (Table 1; all these mutations are localized outside of the CheY-binding domain(s) of FliM^{28,29}). We chose to work with strain SJW2299 [*fliM*(60RC)], which had the highest CW rotation (~95%). In order to examine whether the rotational bias of this strain depends on the presence of CheY, we transduced the selected *fliM* mutation (60RC) from strain SJW2299 into a $\Delta(\textit{cheA-cheZ})$ background (strain SJW3077). The *cheA-cheZ* deletion did not significantly affect the bias of the resulted strain EW193 (compare strains EW193 and SJW2299 in Table 1), indicating that the CW conformation of the mutant protein FliM60RC is independent of the chemotaxis network, including CheY.

We cloned *fliM*_{WT} and *fliM*(60RC) (termed hereinafter *fliM*_{CW}), each with a C-terminal 6 × His tag, within the vector pBAD24, forming the vectors pMWT and pMCW1, respectively. (We have shown earlier that 6 × His-tagged wild-type FliM is phenotypically identical to the tag-free protein.²⁸) FliM expression was under the control of the arabinose pBAD promoter, which had been reported to allow tight regulation of protein

expression.³⁰ Production of plasmid-borne, tagged FliM (FliM_{plasmid}) enabled distinction between chromosomal and plasmid-borne proteins. To examine the modulation level of the plasmid-borne protein, we employed complementation assays under the microscope and on semi-solid agar swarm plates. For this purpose, we transformed wild-type *fliM*, cloned in pBAD24, to the non-flagellated *E. coli fliM* null strain DFB190. Under the microscope, in the absence of arabinose, the cells were completely non-motile. Increasing arabinose levels caused the cells to become motile and then to increase their swimming speed. Above 500 µg/ml, the motility was inhibited (in line with previous observations that overproduction of FliM impairs motility^{31,32}). In semi-solid agar plates, in the absence of arabinose or at low concentrations of arabinose (≤ 1 µg/ml), no swarming was detected. Increasing arabinose concentrations resulted in the formation of expanding rings. An arabinose concentration of 50 µg/ml was the minimal concentration at which three expanding rings, resembling wild-type rings, were observed (not shown). The results of both assays suggest that the chosen expression system allows modulation of FliM expression.

Table 1. Bacterial strains and plasmids used in this study

Strains/plasmids	Relevant genotype	Direction of flagellar rotation of relevant strains ^a	Strain source/reference
A. Strains			
(1) <i>E. coli</i>			
DFB190	<i>fliM</i> null		32
RP437	Wild-type for chemotaxis		50
JM109	Strain for DNA manipulation		51
(2) <i>Salmonella</i>			
SJW3076	$\Delta(\textit{cheA-cheZ})$	0% CW	44
EW191	$\Delta(\textit{cheA-cheZ})\textit{recA}$	0% CW	This study
SJW3077	$\Delta(\textit{fliE-fliN}) \Delta(\textit{cheA-cheZ})$		44
SJW2299	<i>fliM</i> (60RC)	95% CW	52
EW192	<i>fliM</i> (60RC) $\Delta(\textit{cheA-cheZ})$		This study
EW193	<i>fliM</i> (60RC) $\Delta(\textit{cheA-cheZ})\textit{recA}$	89% CW	This study
MY448	<i>fliM</i> (70FL)	37% CW	52
M22	<i>fliM</i> (81VE)	58% CW	44
ST120	<i>fliM</i> (181RH)	84% CW	53
EW194	<i>fliM</i> (181RH) $\Delta(\textit{cheA-cheZ})$	80% CW	This study
M39	<i>fliM</i> (181RP)	33% CW	44
MY1634	<i>fliM</i> (220PL)	0% CW	52
EW195	<i>fliM</i> (220PL) $\Delta(\textit{cheA-cheZ})$		This study
EW196	<i>fliM</i> (220PL) $\Delta(\textit{cheA-cheZ})\textit{recA}$	0% CW	This study
EW197	EW191+pMCW1	Depends on the arabinose level	This study
EW200	EW191+pMCW2	Depends on the arabinose level	This study
EW204	EW193+pMWT	Depends on the arabinose level	This study
EW207	EW196+pMCW1	Depends on the arabinose level	This study
LB5010	(<i>hsdL hsdSA hsdSB</i>) r ⁻ m ⁺		54
LB5010 <i>recA</i>	LB5010 <i>recA</i>		This study
TN2700	TN10dcam with 88% link to <i>recA</i>		The <i>Salmonella</i> Genetic Stock Centre
B. Plasmids			
pBAD24			30
pQE60			QIAGEN
pMCW1	<i>fliM</i> (60RC) cloned in pBAD24		This study
pMCW2	<i>fliM</i> (181RH) cloned in pBAD24		This study
pMWT	<i>fliM</i> (wild-type) cloned in pBAD24		This study

^a Determined in this study.

Flagellar rotation at increasing levels of FliM_{CW}

In order to study the effect of increasing FliM_{CW} levels in the switch on the direction of flagellar rotation, we gradually expressed the protein FliM60RC in a gutted strain containing a wild-type switch-motor complex. The expression was in the strain EW197, which we had constructed by transforming the plasmid pMCW1 into strain EW191 (Table 1). At each level of expression we determined the direction of flagellar rotation and, by Western blot analysis with anti-FliM antibodies, the FliM_{CW}/FliM_{Total} ratio in the whole cell extract.

The dependence of the direction of rotation on the FliM_{CW} level was sigmoidal (Figure 2, circles). A substantial clockwise rotation was obtained not before ~80% of the FliM molecules were FliM_{CW} molecules. Thereafter, the rise in clockwise rotation was very steep. CW rotation of ~50% was obtained when the fraction of FliM_{CW} was ~90% of the total FliM. This suggests that, for 50% probability of shifting the direction of flagellar rotation from CCW to CW, about 31 out of the 35 FliM molecules per switch should be FliM_{CW} molecules. The maximal CW rotation achieved was ~65%; higher FliM_{CW} levels resulted in impaired motility. At an expression level that yields a certain mean percentage of CW rotation, the cells were distributed in a single peak (Figure 3). Single-peak rather than double-peak distribution suggests that the

incorporation of FliM_{Plasmid} was into existing switch complexes. Had the incorporation of FliM_{Plasmid} been mainly to new flagella, we should have observed a large fraction of cells rotating exclusively CCW (existing flagella), and a large fraction of cells rotating predominantly CW (new flagella).

To determine whether or not the FliM_{CW}/FliM_{Total} ratio in the cell truly reflects the FliM_{CW}/FliM_{Total} ratio in the switch, we compared the relative levels of the plasmid-borne FliM_{CW} in whole-cell extracts and in preparations of extended flagellar basal bodies. We determined the total FliM levels in both preparations by a Western blot analysis using an anti-FliM antibody. We likewise determined the levels of the 6 × His-tagged FliM_{Plasmid} in these preparations by a probe specific for the tag. Table 2 shows the results of three different preparations of whole-cell extract isolated from three different bacterial cultures and of their respective preparations enriched with extended flagellar basal bodies. Although the measured FliM_{CW}/FliM_{Total} ratios varied from batch to batch, the relative level of FliM_{CW} in the preparations of extended flagellar basal bodies was not too far from the relative level in the preparations of whole-cell extract. It thus appears that, in first approximation, the FliM_{CW}/FliM_{Total} ratio in the cell correctly reflects the FliM_{CW}/FliM_{Total} ratio in the switch.

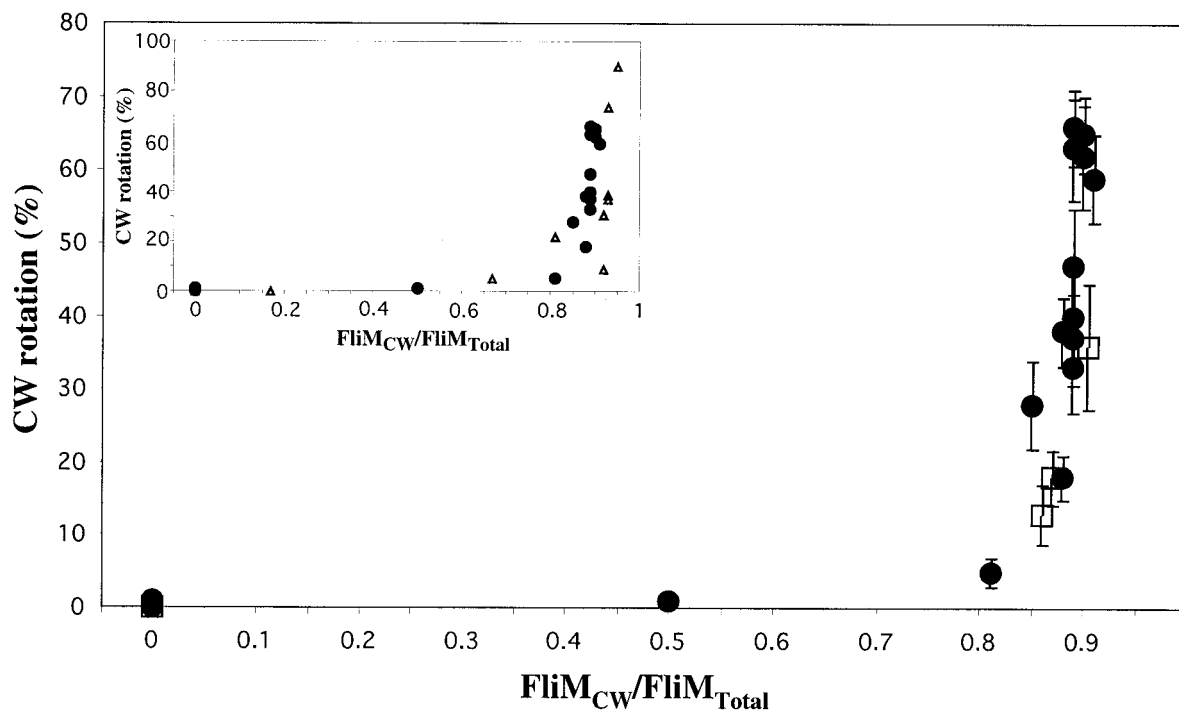


Figure 2. CW rotation as a function of increasing FliM_{CW} levels. Each point is the mean fraction of time spent in CW rotation ± S.E.M. of 10-30 different tethered cells analyzed for about one minute each. Filled circles, EW197 (EW191 expressing FliM60RC); open squares, EW200 (EW191 expressing FliM181RH). Inset, a comparison between the dependence of CW rotation on the relative FliM_{CW} level in a strain containing chromosomal wild-type FliM and a strain containing CCW-mutant FliM (strains EW197 and EW207, respectively). Filled circles, strain EW197; filled triangles, strain EW207.

Table 2. Fraction of plasmid-borne FliM_{CW} in total cell extract and in flagellar basal bodies

Experiment no. ^a	FliM _{CW} /FliM _{Total} ratio in		
	Flagellar basal bodies (%)	Total cell extract (%)	(FliM _{CW} /FliM _{Total} in basal bodies)/ (FliM _{CW} /FliM _{Total} in cell extract)
1	58	41	1.4
2	53	56	0.95
3	74	93	0.80
Average			1.05 ± 0.18 (S.E.M.)

^a Each experiment was carried out with a different batch of bacteria. The strain used was EW197.

To verify that these results are generally correct and are not specific to the pair of proteins employed, we carried out the following two control experiments. In the first experiment, we changed the plasmid-borne protein. Instead of expressing FliM60RC from the plasmid pMCW1, we expressed the CW mutant protein FliM181RH from pMCW2. The experimental points of this protein (open squares in Figure 2) lay well on the original curve of FliM60RC. In the second control experiment, instead of changing the plasmid-borne protein, we changed the host strain (i.e. the chromosomal FliM protein) and expressed FliM60RC in strain EW196, which is a *fliM_{CCW}* mutant. As shown in the inset of Figure 2, the dependence of CW rotation of the new strain (EW207) on the FliM_{CW} level was very similar to that of strain EW197. These control experiments thus suggest that the observed dependence of the direction of rotation on the FliM_{CW} level is general and not specific to the proteins and hosts used.

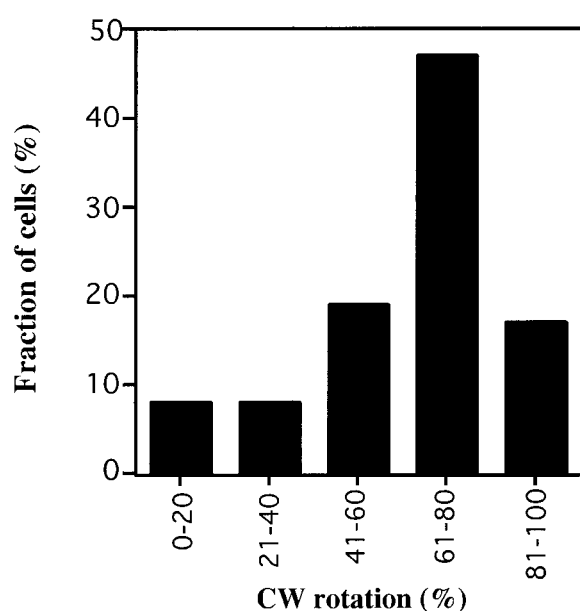


Figure 3. Distribution of CW rotation among different cells. The graph represents the distribution of CW rotation of 36 cells of strain EW197, with an average 61% CW rotation.

Flagellar rotation at increasing levels of FliM_{WT}

In order to study the effect of increasing FliM_{CCW} levels in the switch on the direction of flagellar rotation, we gradually expressed wild-type FliM in a gutted strain of the switch mutant *fliM(60RC)*. (As mentioned above, FliM_{WT} in a gutted background is at the CCW state.) The expression was in strain EW204, which we had constructed by transforming the plasmid pMWT into strain EW193 (Table 1). The CW probability was ~50% when the fraction of FliM_{WT} molecules was 60-70% of the total FliM (shown as 0.3-0.4 FliM_{CW} in Figure 4). Further elevation of the intracellular level of FliM_{WT} to 70-75% (0.25-0.30 FliM_{CW}) reduced the CW rotation to ~10%. A comparison between the increase in FliM_{CW} level in a CCW background (termed hereinafter as the “forward direction”; Figure 2) and the increase in FliM_{CCW} level in a CW background (termed hereinafter as the “reverse direction”; Figure 4), revealed an unexpected result: the forward and reverse processes did not superimpose.

Discussion

The approach taken in this study provided an opportunity to explore, from a new direction, the

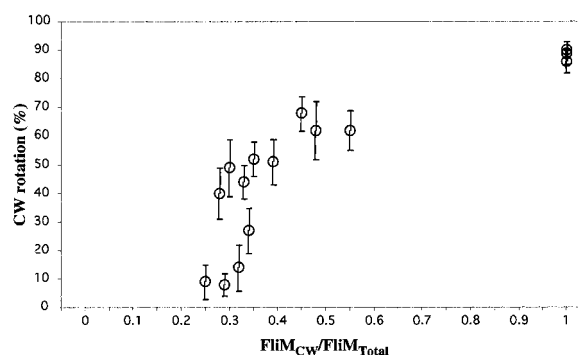


Figure 4. CW rotation in cells expressing increasing levels of FliM_{WT}. For the sake of having a common basis for comparison with Figure 2, the data are presented as a function of FliM_{CW}/FliM_{Total}. FliM_{WT} was expressed from pMWT in a gutted, CW-biased *fliM* mutant (strain EW204). Each point is the mean fraction of time spent in CW rotation ± S.E.M. of 10-30 different tethered cells analyzed for about one minute each.

mechanism of function of the switch, which, hitherto, has been a "black box". The main observations were: (a) a mixture of FliM_{CW} and FliM_{CCW} molecules in the switch can promote an intermediate rotational probability; (b) The CW probability increases from close to zero levels to higher levels only when most of the FliM molecules are in their CW state; (c) once the CW probability rises, it does so with a large gain over a narrow range of FliM_{CW}/FliM_{Total}; (d) an increase in the relative level of FliM_{CW} in the switch is not the inverse of a decrease in this level with respect to the CW probability. Although the interpretation of these findings is not straightforward (see below), the study apparently revealed some new, intriguing features of the mechanism of function of the switch.

Physiological relevance of the results

In this study we made a number of conceptual and technical assumptions. Whether or not the results are physiologically relevant depends on the validity of at least some of these assumptions. Below we list the assumptions and examine their validity.

(a) FliM_{CW} can represent FliM_{WT} occupied by CheY ~ P. This is the basic assumption underlying this study. Currently, in the absence of information on the 3D structures of free and bound FliM, there is no experimental evidence that proves this assumption. However, the finding that the outcome of CheY ~ P binding to FliM is CW rotation^{17,23,25} argues that this assumption is founded and that FliM acquires a high probability of being in the CW state upon CheY ~ P binding. The mutant *fliM*(60RC), which is the origin of the FliM_{CW} protein used here, was chosen out of several tested *fliM* mutants. It is ~90% CW biased at the average (in the absence of CheY; Table 1). This bias is similar to the maximal CW rotation achieved in cells possessing a wild-type switch and containing high levels of active CheY.^{23,24} Thus, as far as we can judge, the assumption that FliM_{CW} represents CheY ~ P-occupied FliM_{WT} is substantiated.

(b) The measured relative level of the plasmid-borne protein in the whole cell reflects its relative level in the switch. Our blotting experiments indeed found comparable relative levels of the plasmid-borne FliM_{CW} in the whole cell extract and in a preparation enriched with flagellar basal bodies (Table 2). This finding holds even though the fraction of flagellar basal bodies was not pure. Had the ratio been different, it should have also been different in a fraction enriched with basal bodies. Moreover, even if the efficiency of incorporation of the plasmid-borne FliM into the switch is only ~80% (the lowest value in Table 2), the results will still hold, with only quantitative differences. Thus, 50% CW probability would be obtained at FliM_{CW}/FliM_{Total} ≈ 0.7 and 0.4-0.5

(instead of 0.9 and 0.3-0.4) for the forward and reverse directions, respectively

(c) FliM_{Plasmid} is, to a first approximation, evenly distributed among different flagella. The validity of this assumption depends on even expression of FliM_{Plasmid} in the cells and on its even distribution among different flagella. Here we used the arabinose pBAD expression system, because of its tight regulation and modulation.³⁰ At the onset of this project and later towards its end, studies were published, suggesting that the arabinose levels and, consequently, the extent of protein expression from the pBAD system in *E. coli* cells are not evenly distributed among different cells.^{33,34} These studies proposed that the average increase in the expression level over a bacterial population is mainly due to an increased number of cells expressing high protein levels rather than the consequence of increased protein levels in individual cells. This phenomenon was attributed to the inducible L-arabinose transport system^{33,34}, which includes the low affinity permease (encoded by the *araE* gene) and the high affinity system specified by the *araFG* operon³⁵. In *Salmonella* the situation may be different, because the high-affinity transport system is missing.³⁵ The single peak distribution of CW rotation given in Figure 3 suggests that, in our experimental system, the situation is indeed different and that FliM_{Plasmid} expression in the cells is rather homogeneous. The similarity between the relative level of FliM_{Plasmid} in the switch and the total cell extract, taken together with the single peak distribution of CW rotation, further argues that there is an efficient equilibrium between cytoplasmic and flagellar FliM in the cells. This suggests that the heterogeneity of the FliM_{Plasmid} level among different flagella is not larger than among different cells.

It thus seems that the assumptions made are valid and the results are physiologically relevant, at least from a qualitative point of view. The quantitative aspect depends on the accuracy of the determination of the protein levels by blotting. Regrettably, this method is not always sufficiently reproducible and the results of different blots may vary. We tried to reduce the variation by determining the relative levels of the different FliM forms rather than the absolute levels. Thus, in each experiment we compared in the same blot the cellular chromosomal and plasmid-borne levels of FliM. Furthermore, in each preparation of flagellar basal bodies we compared, on the same blot, the FliM levels in the basal body fraction and the FliM levels in the whole cell extract. Quantitatively, however, we regard the results as an approximation.

Characteristics of CW generation at the switch

Each FliM molecule forms a complete CheY-binding site.²⁸ Assuming that FliM_{CW} can represent FliM_{WT} occupied by CheY ~ P, the following conclusions can be made on the basis of our results.

When the relative level of FliM occupancy by CheY ~ P (equivalent, according to the assumption, to $FliM_{CW}/FliM_{Total}$) gradually increases, the probability of CW rotation does not significantly increase before a substantial fraction of the FliM molecules become occupied. Thus, to the first approximation, about 31 of the 35 FliM molecules in a given switch should apparently be occupied for 50% probability of CW rotation.

As the relative level of FliM occupancy by CheY ~ P increases, once the rise in CW rotation starts, it is very steep, i.e. CW rotation is gained over an extremely narrow range of occupancy. Since the rise starts not before the relative occupancy level is ~80% (Figure 2), a question arises whether the observed steepness is an inevitable outcome of the narrow range available for the rise. While this possibility might contribute to the steepness, it does not seem to be the only cause. This is because the reverse process is moderately steep in spite of the relatively wide range available for the decrease in occupancy (Figure 4).

The steepness, found here, is in line with earlier studies, which found a steep dependence of the degree of CW rotation on the intracellular concentration of active CheY.²²⁻²⁵ It was suggested that the mechanism of switching involves cooperativity of CheY binding to the switch^{3,22,25,36} or cooperativity of post-binding interactions among subunits of the switch.³⁶ The studies, which measured the dependence of the CW rotation on the intracellular concentration of active CheY, could not distinguish between these possibilities. This study, which bypassed the binding step, suggests that post-binding processes within the switch are cooperative.

Increasing versus decreasing switch occupancy

A surprising observation made in this study is that the forward and reverse processes of modulating the relative level of $FliM_{CW}$ in the switch did not superimpose (Figure 2 versus Figure 4). Assuming that $FliM_{CW}$ can represent $FliM_{WT}$ occupied by CheY ~ P, this suggests that the changes in CW probability, observed when the occupancy of FliM increases and decreases, are not reciprocal. This observation might be meaningful for the mechanism of switching only if a substitution of $FliM_{CCW}$ for $FliM_{CW}$ (and *vice versa*) took place. As discussed above, our observation that the distribution of CW-rotating cells had only a single peak (Figure 3) suggests that such substitution indeed occurred. Another question, for which we do not have an answer, is whether a slow incorporation of newly formed $FliM_{CW}$ or $FliM_{CCW}$ molecules into the switch is comparable to the fast changes in the occupancy of existing FliM molecules by CheY ~ P. If such a comparison is valid and meaningful, our results suggest the occurrence of a hitherto unknown phenomenon: a change in the CW probability, which evolves from increased occupancy, is not

the reverse of a change, which evolves from decreased occupancy.

This hysteresis-like phenomenon is consistent with stochastic simulations of CheY ~ P fluctuations in the cell, carried out by Morton-Firth & Bray.³⁷ These simulations did not support a simple threshold-crossing mechanism for switching, but rather a two-threshold mechanism: one threshold for CCW-to-CW switching upon CheY ~ P elevation, and a different threshold for CW-to-CCW switching upon a decrease in CheY ~ P level.

Hysteresis is a well-known phenomenon in physics. It also occurs in a number of biological systems such as the Ca^{2+} channel of the skeletal muscle ryanodine receptor, which exhibits a pronounced hysteresis to changes in pH,³⁸ the porin channel, which manifests a clear hysteresis in current-voltage diagrams,^{39,40} and muscles, which demonstrate hysteresis in length-tension loops during contraction and release.^{41,42}

How can such a hysteresis-like phenomenon happen in the switch? We can imagine a situation, similar to that proposed by Walz & Caplan,⁴³ in which the switch can be in multiple states. The switch undergoes a polymorphic transition, the extent of which depends on the occupancy of FliM by CheY ~ P and the CW probability of the motor is accordingly determined. The observed hysteresis-like phenomenon suggests that a given CW probability can occur at different occupancy levels of the switch, depending on the route by which they were created. This dependence on the route might be a reflection of the different energy barriers for the polymorphic transitions upon increasing and decreasing occupancy of FliM.

What is the advantage given to the switch and to the cell by hysteresis? The very steep dependence of CW rotation on the CheY ~ P level, which was revealed by Cluzel *et al.*²⁵ when studying individual cells, raised the suggestion "that an additional molecular mechanism to adjust [CheY ~ P] within the (extremely narrow) operational range of the motors will exist".²⁵ If a hysteresis-like phenomenon is indeed involved in switching and there is a difference between the thresholds of the forward and reverse processes, it may provide such a mechanism. This is exemplified in Figure 5, which shows hypothetical random fluctuations of CheY ~ P (lower panel) and the resulting probability of CW rotation (upper panel). As long as the CheY ~ P fluctuations are below the CW threshold, the probability of CW rotation would be very low and the motor would rotate CCW. Only when the CheY ~ P level exceeds this threshold, the CW probability would increase. High probability of CW rotation would not be terminated as soon as the CheY ~ P level returns to below this threshold. The CheY ~ P level should go to below the lower CCW threshold in order to reverse the direction of rotation. This proposed mechanism, which is essentially a damping mechanism, stabilizes the probability of rotation in each

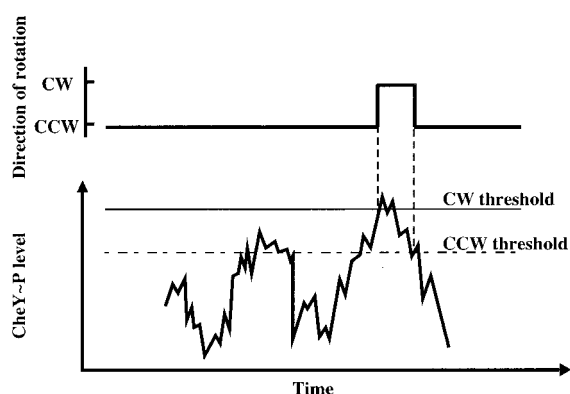


Figure 5. Schematic presentation of the potential role of the different thresholds of CheY ~ P for CW and CCW rotation. Lower panel, hypothetical random fluctuations in CheY ~ P levels (based on Figure 3 of Morton-Firth & Bray³⁷). Upper panel, direction of flagellar rotation as a result of changes in CheY ~ P levels. See the text for details.

direction and prevents a situation, in which CheY ~ P fluctuations would instantaneously be reflected in the direction of flagellar rotation and, hence, in the bacterial swimming mode.

Materials and Methods

Bacteria and plasmids

The bacterial strains and plasmids used in this study are listed in Table 1. The strains EW192 and EW195 were generated by transducing their *fliM* mutation [*fliM*(60RC) and *fliM*(220PL), respectively] into the non-flagellated and chemotactically gutted strain SJW3077. Transduction was carried out with P22 according to Magariyama *et al.*⁴⁴ The *cheA-cheZ* deletion was confirmed by PCR, carried out with primers for the N and C termini of the *cheY* gene. In both strains no PCR product was obtained, in contrast to the parent strains SJW2299 and MY1634. As an additional positive control, we carried out PCR with primers for the N and C termini of the *fliM* gene. A PCR product was obtained in all strains. The host strains EW191, EW193, and EW196 were generated by P22 transduction of a *recA* mutation from TN2700 to SJW3076, EW192, and EW195, respectively, in order to prevent recombination between the plasmid-originated and chromosomal copies of *fliM*.

The presence of the *recA* deficiency was assayed by sensitivity to UV radiation as follows. Several chloramphenicol (Cap)-resistance colonies, obtained by the transduction, were grown in Luria-broth (LB) to $A_{590} \approx 0.5$. (Since the marker Cap was linked to the *recA* mutation, selection for positive transductants was carried out on Cap-containing plates.) Aliquots of 20 μ l from each culture were inoculated as a line on LB plates. The plates were irradiated by different dosages of UV light and incubated at 35 °C. Cultures which showed elevated sensitivity for the UV radiation were selected.

Wild-type *fliM*, *fliM*(60RC), and *fliM*(120RH) were amplified from the chromosomal DNA of strains SJW3076, SJW2299 and ST120, respectively. The 5' pri-

mer contained an added *NcoI* site while the 3' primer contained an added *BglII* site. The amplified *fliM*-containing fragments were digested with *NcoI* and *BglII* and ligated with pQE60 (containing the coding region for six histidine residues downstream to the *BglII* site), pre-digested with the same enzymes. The resulting plasmids were digested with *NcoI* and *HindIII* (*HindIII* resides downstream to the coding region for the six histidine residues). The *fliM*- and 6 \times His-tag-containing fragments were ligated with pBAD24, pre-digested with the same enzymes, and transformed to the *E. coli* strain JM109. To prevent digestion of the plasmids in the final *Salmonella* hosts, the plasmids were transformed to the *Salmonella* strain LB5010*recA*, which is r^-m^+ for all three chromosomal systems of DNA restriction and modification. Subsequently, the plasmids were transformed to their final hosts: pMWT to EW193 (generating the strain EW204), pMCW1 to EW191 and EW196 (generating the strains EW197 and EW207, respectively), and pMCW2 to EW191 (generating the strain EW200).

Cell cultures

The strains EW197, EW200, EW204 and EW207 were grown overnight at 35 °C in M9 medium supplemented with 0.5% (w/v) Casamino acids, 0.5% (v/v) glycerol, 5 μ g/ml thiamine and 100 μ g/ml ampicillin. The cultures were diluted 75-fold in the same medium and grown to $A_{590} \approx 0.1$ at 35 °C. Each culture was divided to portions, and each portion was grown to $A_{590} = 0.5-0.6$ in the presence of a different L-arabinose concentration (ranging from 0 to 1 mg/ml). Each sub-culture was used both for quantification of FliM and for determination of the direction of flagellar rotation. For the preparation of extended flagellar basal bodies, an overnight culture of strain EW197 was diluted 75-fold into 1.5 l of the same medium, grown as described above, and induced with 100 μ g/ml arabinose.

Determination of the direction of flagellar rotation

The direction of flagellar rotation was monitored by the tethering technique.²¹ Cells, washed and resuspended in motility buffer (20 mM Tris-HCl (pH 7.5), 0.1 mM EDTA), were tethered as described,⁴⁵ using a flow chamber.⁴⁶ The rotation of the tethered cells was recorded on a VCR at 50 frames/second. The recordings were analyzed by a computerized motion analysis system (Hobson Rotation Tracking System, England). The output of this system was a sequential list of the time intervals in the three rotational states: CW, CCW and a pause. Another software (Event.exe, obtained from M. D. Levin) used the raw data from the Hobson Rotation Tracking System and calculated, for each cell, the fractional CCW rotation, CW rotation and pausing. In most cases, the average pausing time (usually $\sim 10\%$ of the time) remained essentially unchanged with the induction level of FliM. In these cases we considered only two states, CW and CCW. In the few cases in which the pause time significantly increased with the $FliM_{CW}$ level, the added pausing time was considered as a futile switching event¹⁸ and was added to the relative time spent in CW rotation.

Isolation of extended flagellar basal bodies

Basal flagellar fragments were prepared from strain EW197 according to Zhao *et al.*⁴⁷ and Francis *et al.*⁴⁸

with several modifications. The bacteria were harvested, washed once, and resuspended in buffer A (10 mM Tris-HCl (pH 7.9), 50 mM NaCl). Following one minute blending, the bacteria were spun-down and the pellet stored frozen at -20°C . For the isolation, the pellet was resuspended to homogeneity in 70 ml of buffer B (500 mM sucrose, 10 mM Tris-HCl (pH 7.9), 0.2 mM phenylmethylsulfonyl fluoride (PMSF)), followed by addition of lysozyme (0.1 mg/ml final concentration, from a freshly prepared stock solution) and EDTA (10 mM). The solution was gently stirred at 35°C for about two hours, until a large fraction of the cells became spheroplasts. Triton X-100 (0.2% (v/v) final concentration) was added to lyse the spheroplasts. When the lysis was complete, MgSO_4 (10 mM final concentration) was added for DNA degradation and the solution was gently stirred at 35°C for 30 minutes. Unlysed cells and cell debris were removed by centrifugation at 3000 g for 15 minutes. Inclusion bodies were removed at $15,000\text{ g}$ for 20 minutes. The pH of the supernatant was raised with 5 M NaOH to $\sim\text{pH } 10$. Membranes were pelleted by high-speed centrifugation ($60,000\text{ g}$ for one hour at 4°C). The pellet was resuspended in 1 ml buffer C (10 mM Tris-HCl (pH 7.9), 5 mM EDTA, 0.1% (v/v) Triton X-100, 0.2 mM PMSF). Following the addition of 1 ml of 20% (v/v) Triton X-100, the suspension was passed back-and-forth (at least ten times) through a 24-gauge needle. The resulting solution was diluted in 18 ml of buffer C. After low-speed centrifugation ($15,000\text{ g}$ for 20 minutes at 4°C), the flagella were pelleted by high-speed centrifugation ($60,000\text{ g}$ for one hour at 4°C) and resuspended in 500 μl of buffer C. The resulting preparation, enriched with basal flagellar fragments, was negatively stained with 1% (w/v) uranyl acetate and visualized with an electron microscope.

FliM quantification

In whole cells

Aliquots containing a constant number of bacteria ($\sim 3 \times 10^8$ cells (based on 4×10^8 to 8×10^8 cells/ml at $A_{600} = 1$)⁴⁹) were pelleted, resuspended in 50 μl of SDS sample buffer, boiled for ten minutes, and kept at -20°C . Samples (10 μl from each aliquot) were resolved on SDS-12% (w/v) PAGE and transferred to nitrocellulose membranes (0.2 μm ; Schleicher & Schuell) with a Mini Trans-Blot Electrophoretic Transfer Cell (BioRad). The membranes were blocked overnight at 4°C with 5% (w/v) milk, 10 mM Tris-HCl (pH 7.5), 15 mM NaCl, 0.05% (v/v) Tween 20, and then sequentially probed with polyclonal anti-FliM antibody (a gift from S. I. Aizawa) and peroxidase-conjugated anti-rabbit antibody (Sigma). The immunoblots were assayed with Super-Signal chemiluminescent substrate (Pierce), and exposed to SuperRX films (Fuji). Films were scanned with an imaging densitometer (model GS-690, BioRad), and the intensities of the bands were quantified by the Multi-Analyst software (BioRad). The intensity of the FliM bands represented the total FliM level in the sample (both endogenous and induced). The relative level of the induced protein (expressed as $\text{FliM}_{\text{CW}}/\text{FliM}_{\text{Total}}$ or $\text{FliM}_{\text{WT}}/\text{FliM}_{\text{Total}}$) was calculated for each sample based on the intensity of the FliM band in the induced and non-induced samples.

In preparations of flagellar basal bodies from strain EW197

The total protein concentrations in the cell extract and flagellar-pellet fractions were determined by the BCA Protein Assay kit (Pierce). Equal protein amounts from each fraction (2-10 μg , in 20 μl samples) were prepared for gel electrophoresis together with known amounts (10-200 ng) of purified 6 \times His-FliM. Quantities of 5 μl of fivefold concentrated SDS sample buffer were added to the samples, which were then boiled for ten minutes. Sample duplicates were run on two parallel SDS-12% PAGE. The proteins were transferred to nitrocellulose membranes and blocked as described above. One membrane was reacted as described above with anti-FliM antibodies to determine the total FliM level in the fraction. The other membrane was reacted with an INDIA HisProbe-HRP reagent (Pierce) to determine the level of the 6 \times His-tagged, plasmid-borne protein. The nitrocellulose membranes were assayed and analyzed as described above. FliM levels (total or plasmid-borne FliM) in the different fractions were determined according to a standard curve of purified proteins on the same membrane.

Acknowledgements

We thank Y. Blat for raising the idea underlying this study, U. Alon for a helpful discussion, D. Bray for proposing Figure 5, and H. C. Berg for comments on an early version of the manuscript. We are grateful to S. R. Caplan for indicating to us that the results of Figure 2 *versus* Figure 4 reflect hysteresis of the switch, and for raising the idea that the switch might be in multiple states and might undergo a polymorphic transition between them. S.-I. Aizawa is acknowledged for anti-FliM antibodies, D. F. Blair, R. B. Bourret, R. M. Macnab and S. Yamaguchi for bacterial strains and plasmids, M. D. Levin for software for calculating the rotational bias of tethered cells, and Y. Marikovsky for help with the electron microscope. M.E. is an incumbent of Jack and Simon Djanogly Professorial Chair in Biochemistry. The study was supported by grant number 96-00013 from the United States-Israel Binational Science Foundation (BSF) and 111/99 from the Israel Science Foundation.

References

1. Macnab, R. M. (1996). Flagella and motility. In *Escherichia coli and Salmonella: Cellular and Molecular Biology* (Neidhardt, F. C., Curtis, R., III, Ingraham, J. L., Lin, E. C. C., Low, K. B., Magasanik, B., Reznikoff, W. S., Riley, M., Schaechter, M. & Umberger, H. E., eds), 2nd edit., pp. 123-145, American Society for Microbiology, Washington, DC.
2. Larsen, S. H., Reader, R. W., Kort, E. N., Tso, W.-W. & Adler, J. (1974). Change in direction of flagellar rotation is the basis of the chemotactic response in *Escherichia coli*. *Nature*, **249**, 74-77.
3. Macnab, R. M. (1995). Flagellar switch. In *Two-Component Signal Transduction* (Hoch, J. A. & Silhavy, T. J., eds), pp. 181-199, American Society for Microbiology, Washington, DC.

4. Zhao, R. B., Amsler, C. D., Matsumura, P. & Khan, S. (1996). FliG and FliM distribution in the *Salmonella typhimurium* cell and flagellar basal bodies. *J. Bacteriol.* **178**, 258-265.
5. Thomas, D. R., Morgan, D. G. & DeRosier, D. J. (1999). Rotational symmetry of the C ring and a mechanism for the flagellar rotary motor. *Proc. Natl Acad. Sci. USA*, **96**, 10134-10139.
6. Zhao, R. H., Pathak, N., Jaffe, H., Reese, T. S. & Khan, S. (1996). FliN is a major structural protein of the c-ring in the *Salmonella typhimurium* flagellar basal body. *J. Mol. Biol.* **261**, 195-208.
7. Eisenbach, M. & Adler, J. (1981). Bacterial cell envelopes with functional flagella. *J. Biol. Chem.* **256**, 8807-8814.
8. Parkinson, J. S. & Houts, S. E. (1982). Isolation and behavior of *Escherichia coli* deletion mutants lacking chemotaxis functions. *J. Bacteriol.* **151**, 106-113.
9. Eisenbach, M. (1996). Control of bacterial chemotaxis. *Mol. Microbiol.* **20**, 903-910.
10. Stock, J. B. & Surette, M. G. (1996). Chemotaxis. In *Escherichia coli and Salmonella: Cellular and Molecular Biology* (Neidhardt, F. C., Curtis, R., III, Ingraham, J. L., Lin, E. C. C., Low, K. B., Magasanik, B., Reznikoff, W. S., Riley, M., Schaechter, M. & Umberger, H. E., eds), 2nd edit., pp. 1103-1129, American Society for Microbiology, Washington, DC.
11. Falke, J. J., Bass, R. B., Butler, S. L., Chervitz, S. A. & Danielson, M. A. (1997). The two-component signaling pathway of bacterial chemotaxis: a molecular view of signal transduction by receptors, kinases, and adaptation enzymes. *Annu. Rev. Cell Dev. Biol.* **13**, 457-512.
12. Bren, A. & Eisenbach, M. (2000). How signals are heard during bacterial chemotaxis: protein-protein interactions in sensory signal propagation. *J. Bacteriol.* **182**, 6865-6873.
13. Hess, J. F., Oosawa, K., Matsumura, P. & Simon, M. I. (1987). Protein phosphorylation is involved in bacterial chemotaxis. *Proc. Natl Acad. Sci. USA*, **84**, 7609-7613.
14. Hess, J. F., Oosawa, K., Kaplan, N. & Simon, M. I. (1988). Phosphorylation of three proteins in the signaling pathway of bacterial chemotaxis. *Cell*, **53**, 79-87.
15. Wylie, D., Stock, A., Wong, C.-Y. & Stock, J. (1988). Sensory transduction in bacterial chemotaxis involves phosphotransfer between Che proteins. *Biochem. Biophys. Res. Commun.* **151**, 891-896.
16. Welch, M., Oosawa, K., Aizawa, S.-I. & Eisenbach, M. (1993). Phosphorylation-dependent binding of a signal molecule to the flagellar switch of bacteria. *Proc. Natl Acad. Sci. USA*, **90**, 8787-8791.
17. Barak, R. & Eisenbach, M. (1992). Correlation between phosphorylation of the chemotaxis protein CheY and its activity at the flagellar motor. *Biochemistry*, **31**, 1821-1826.
18. Eisenbach, M., Wolf, A., Welch, M., Caplan, S. R., Lapidus, I. R. & Macnab, R. M. *et al.* (1990). Pausing, switching and speed fluctuation of bacterial flagellar motor and their relation to motility and chemotaxis. *J. Mol. Biol.* **211**, 551-563.
19. Macnab, R. M. (1977). Bacterial flagella rotating in bundles: A study in helical geometry. *Proc. Natl Acad. Sci. USA*, **74**, 221-225.
20. Macnab, R. M. & Ornston, M. K. (1977). Normal-to-curlly flagellar transitions and their role in bacterial tumbling: stabilization of an alternative quaternary structure by mechanical force. *J. Mol. Biol.* **112**, 1-30.
21. Silverman, M. & Simon, M. (1974). Flagellar rotation and the mechanism of bacterial motility. *Nature*, **249**, 73-74.
22. Kuo, S. C. & Koshland, D. E., Jr (1989). Multiple kinetic states for the flagellar motor switch. *J. Bacteriol.* **171**, 6279-6287.
23. Alon, U., Camarena, L., Surette, M. G., Arcas, B. A. Y., Liu, Y., Leibler, S. & Stock, J. B. (1998). Response regulator output in bacterial chemotaxis. *EMBO J.* **17**, 4238-4248.
24. Scharf, B. E., Fahrner, K. A., Turner, L. & Berg, H. C. (1998). Control of direction of flagellar rotation in bacterial chemotaxis. *Proc. Natl Acad. Sci. USA*, **95**, 201-206.
25. Cluzel, P., Surette, M. & Leibler, S. (2000). An ultra-sensitive bacterial motor revealed by monitoring signaling proteins in single cells. *Science*, **287**, 1652-1655.
26. Aizawa, S. & Kubori, T. (1998). Bacterial flagellation and cell division. *Genes Cells*, **3**, 625-634.
27. Wolfe, A. J., Conley, M. P. & Berg, H. C. (1988). Acetyladenylyate plays a role in controlling the direction of flagellar rotation. *Proc. Natl Acad. Sci. USA*, **85**, 6711-6715.
28. Bren, A. & Eisenbach, M. (1998). The N terminus of the flagellar switch protein, FliM, is the binding domain for the chemotactic response regulator, CheY. *J. Mol. Biol.* **278**, 507-514.
29. Mathews, M. A. A., Tang, H. L. & Blair, D. F. (1998). Domain analysis of the FliM protein of *Escherichia coli*. *J. Bacteriol.* **180**, 5580-5590.
30. Guzman, L.-M., Belin, D., Carson, M. J. & Beckwith, J. (1995). Tight regulation, modulation, and high-level expression by vectors containing the arabinose P_{BAD} promoter. *J. Bacteriol.* **177**, 4121-4130.
31. Clegg, D. O. & Koshland, D. E., Jr (1985). Identification of a bacterial sensing protein and effects of its elevated expression. *J. Bacteriol.* **162**, 398-405.
32. Tang, H. & Blair, D. F. (1995). Regulated underexpression of the FliM protein of *Escherichia coli* and evidence for a location in the flagellar motor distinct from the MotA/MotB torque generators. *J. Bacteriol.* **177**, 3485-3495.
33. Siegele, D. A. & Hu, J. C. (1997). Gene expression from plasmids containing the araBAD promoter at subsaturating inducer concentrations represents mixed populations. *Proc. Natl Acad. Sci. USA*, **94**, 8168-8172.
34. Khlebnikov, A., Risa, O., Skaug, T., Carrier, T. A. & Keasling, J. D. (2000). Regulatable arabinose-inducible gene expression system with consistent control in all cells of a culture. *J. Bacteriol.* **182**, 7029-7034.
35. Lin, E. C. C. (1996). Dissimulatory pathways for sugars, polyols, and carboxylates. In *Escherichia coli and Salmonella: Cellular and Molecular Biology* (Neidhardt, F. C., Curtis, R., III, Ingraham, J. L., Lin, E. C. C., Low, K. B., Magasanik, B., Reznikoff, W. S., Riley, M., Schaechter, M. & Umberger, H. E., eds), 2nd edit., pp. 307-342, American Society for Microbiology, Washington, DC.
36. Spiro, P. A., Parkinson, J. S. & Othmer, H. G. (1997). A model of excitation and adaptation in bacterial chemotaxis. *Proc. Natl Acad. Sci. USA*, **94**, 7263-7268.
37. Morton-Firth, C. J. & Bray, D. (1998). Predicting temporal fluctuations in an intracellular signalling pathway. *J. Theoret. Biol.* **192**, 117-128.

38. Ma, J. & Zhao, J. (1994). Highly cooperative and hysteretic response of the skeletal muscle ryanodine receptor to changes in proton concentrations. *Biophys. J.* **67**, 626-633.
39. Mathes, A. & Engelhardt, H. (1998). Voltage-dependent closing of porin channels: analysis of relaxation kinetics. *J. Membr. Biol.* **165**, 11-18.
40. Schindler, H. & Rosenbusch, J. P. (1981). Matrix protein in planar membranes: clusters of channels in a native environment and their functional reassembly. *Proc. Natl Acad. Sci. USA*, **78**, 2302-2306.
41. Kostyukov, A. I. & Cherkassky, V. L. (1992). Movement-dependent after-effects in the firing of the spindle endings from the de-efferented muscles of the cat hindlimb. *Neuroscience*, **46**, 989-999.
42. Cherkassky, V. L. (1997). After-effects of preceding movement on dynamic responses of spindle primary afferents during passive muscle lengthening in the cat. *Neuroscience*, **76**, 611-617.
43. Walz, D. & Caplan, S. R. (2000). An electrostatic mechanism closely reproducing observed behavior in the bacterial flagellar motor. *Biophys. J.* **78**, 626-651.
44. Magariyama, Y., Yamaguchi, S. & Aizawa, S.-I. (1990). Genetic and behavioral analysis of flagellar switch mutants of *Salmonella typhimurium*. *J. Bacteriol.* **172**, 4359-4369.
45. Ravid, S. & Eisenbach, M. (1983). Correlation between bacteriophage *chi* adsorption and mode of flagellar rotation of *Escherichia coli* chemotaxis mutants. *J. Bacteriol.* **154**, 604-611.
46. Berg, H. C. & Block, S. M. (1984). A miniature flow cell designed for rapid exchange of media under high-power microscope objectives. *J. Gen. Microbiol.* **130**, 2915-2920.
47. Zhao, R. B., Schuster, S. C. & Khan, S. (1995). Structural effects of mutations in *Salmonella typhimurium* flagellar switch complex. *J. Mol. Biol.* **251**, 400-412.
48. Francis, N. R., Sosinsky, G. E., Thomas, D. & DeRosier, D. J. (1994). Isolation, characterization and structure of bacterial flagellar motors containing the switch complex. *J. Mol. Biol.* **235**, 1261-1270.
49. Adler, J. (1973). A method for measuring chemotaxis and use of the method to determine optimum conditions for chemotaxis by *Escherichia coli*. *J. Gen. Microbiol.* **74**, 77-91.
50. Parkinson, J. S. (1978). Complementation analysis and deletion mapping of *Escherichia coli* mutants defective in chemotaxis. *J. Bacteriol.* **135**, 45-53.
51. Yanisch-Perron, C., Vieira, J. & Messing, J. (1985). Improved M13 phage cloning vectors and host strains: nucleotide sequence of the M13mp18 and pUC19 vectors. *Gene*, **33**, 103-119.
52. Sockett, H., Yamaguchi, S., Kihara, M., Irikura, V. M. & Macnab, R. M. (1992). Molecular analysis of the flagellar switch protein FliM of *Salmonella typhimurium*. *J. Bacteriol.* **174**, 793-806.
53. Rubik, B. A. & Koshland, D. E., Jr (1978). Potentiation, desensitization and inversion of response in bacterial sensing of chemical stimuli. *Proc. Natl Acad. Sci. USA*, **75**, 2820-2824.
54. Bullas, L. R. & Ryu, J.-I. (1983). *Salmonella typhimurium* LT2 strains which are r^-m^+ for all three chromosomally located systems of DNA restriction and modification. *J. Bacteriol.* **156**, 471-474.

Edited by B. Holland

(Received 30 March 2001; received in revised form 22 July 2001; accepted 6 August 2001)